Effect of Chemical Composition on the Microstructure, Hardness and Electrical Conductivity Profiles of the Ag-Bi-Ge Alloys

Aleksandar Marković[a], Duško Minić[a], Milena Premović[a]* Dragan Manasijević[b], Dejan Guresić[a]

and Milan Kolarevi[c]

[a]Faculty of Technical Science, University of Priština, Kneza Miloša 7, 28320 Kos. Mitrovica, Serbia
[b]Technical Faculty in Bor, University of Belgrade, VJ 12, 19210 Bor, Serbia
[c]Faculty of Mechanical Engineering, University of Kragujevac, Kraljevo, Serbia

Microstructure, hardness and electrical properties of the selected ternary Ag-Bi-Ge alloys were investigated in this study. Isothermal sections of the Ag-Bi-Ge system at 25, 100 and 500 °C have been extrapolated using optimized thermodynamic parameters from literature and experimentally investigated. Performed experiments were optical microscopy, scanning electron microscopy (SEM) and energy dispersive spectrometry (EDS), X-ray powder diffraction (XRD), hardness measurements by Brinell method and electrical conductivity measurements. EDS results were compared with predicted phase equilibria and good overall agreement between experimental and calculated values was obtained. XRD results were also in agreement with predicted phase equilibria. Hardness and electrical conductivity of selected alloys were measured and by using appropriated mathematical model these properties were predicted in the whole composition range.

Keywords: *Phase equilibrium, hardness, electrical conductivity, mathematical model.*

1. Introduction

Due to the high requirement of the computer market and customers, improvements of the computational performance are very demanding. Some of demands are fast starting of computers or laptops and being ready for operation in less than a second, and storing large amounts of data in a very small space. Due to the these requirements it is necessary to develop a universal memory that can read, write, and erase data at high speed, as well as using little power with reasonable development and production costs. Germanium based alloys are essential in the modern technology for making memory materials and for the production of DVDs, optical, flash and Blue-Ray disks, etc. First Ge15Sb85 [1] alloy was fabricated as a useful memory material, but improving the high thermal stability of these alloys was still necessary. So, Ge-Sb alloys were doped with Te [2-6] and ternary alloys such as Ge1Sb4Te7, Ge1Sb2Te4, Ge2Sb2Te5, and Ge3Sb2Te6 were selected as potential phase-change materials. The ternary alloy Ge2Sb2Te5 was shown to be most favorable for use in memory devices. This ternary alloy is suitable because the switch time is much faster but disadvantage is low temperature of crystallization so, further investigations are needed in this area. On the other hand, silver, germanium, bismuth [7-13] and their respective alloys are becoming of increasing importance in the electronics industry due to their favorable thermal and electrical properties. Due to the wide possible applications of the silver, germanium, and bismuth based alloys, it is a matter of high importance to investigate the multicomponent alloys based on the Ag-Ge-Bi.

Second reason for testing these alloys is due to the limited number of research of Ag-Ge-Bi based alloys [14-16]. Results presented in this study should benefit to the industry for designing and developing new alloys.

The ternary Ag-Bi-Ge system has been experimental and analytically investigated previously by our group [17]. Investigated samples were from three vertical sections and two isothermal sections at 200 and 400 °C. As a result reliable thermodynamic data set has been proposed.

Based on results from previous study [17], thermodynamic data set has been used in current study for calculation of the isothermal sections at 25, 100 and 500 °C. Phase equilibria of the isothermal sections at 25, 100 and 500 °C were checked by using scanning electron microscopy (SEM) with energy dispersive spectrometry (EDS), X-ray powder diffraction (XRD) analysis and inverted metallographic microscope. For better insight into the properties of the Ag-Bi-Ge alloys, hardness and electrical conductivity were investigated in the current study. Based on experimental results and by using appropriated mathematical model these properties were predicted along whole composition range.

2. Materials and Methods

High-purity Ag (99.999 at. %), Bi (99.999 at. %) and Ge (99.999 at. %) produced by Alfa Aesar (Germany) were used for preparation of investigated alloys. Used elements were carefully measured in different molar ratio.

*e-mail: milena.premovic@gmail.com

Total mass of each samples were 3 g. Such samples were melted and re-melted five times in an induction furnace under high purity Ar atmosphere. The average weight loss of the samples during melting was about 1 mass %. After melting samples were divided into three series. Samples for investigation of isothermal sections at 500 °C and 100 °C, were sealed in evacuated quartz tubes and then heated to a temperature that is 50 °C higher than the melting temperature of Ag. The alloy samples were then cooled down to 500 °C (one series) and 100 °C (another series) at the cooling rate of 5 °Cmin⁻¹. The samples were kept at 500 °C for four weeks and seven weeks at 100 °C and then quenched in the water and ice mixture to preserve desired equilibrium at 500 and 100 °C. These samples were used for SEM-EDS and XRD analysis. The compositions of the samples and phases presented in samples were determined using a JEOL JSM-6460 scanning electron microscope (SEM) which was equipped with an EDS system (Oxford Instruments X-act). The samples for SEM-EDS analysis were ground using sand paper, polished with diamond paste, and then cleaned in an ultrasonic bath. The overall compositions of the annealed samples were determined by mapping the entire polished surfaces of the samples. By contrast, the compositions of the observed coexisting phases were determined examining the surface of the same phase at different parts of the sample (at least five different positions of the same phase were examined per phase). The chemical compositions of the phases determined in this study represented the mean values based on at least five individual analyses. Powder XRD data for the phase analysis of the alloy samples were recorded with a D2 PHASER (Bruker, Karlsruhe, Germany) powder diffractometer equipped with a dynamic scintillation detector and ceramic X-ray Cu tube (KFL-Cu-2K) in the 2θ range from 10° to 75° with a step size of 0.02°. Before the XRD analysis, the selected samples were first powdered using ball mill (YKT-04 machine) and the powders obtained were then placed in special holders and pressed to obtain compact samples. The recorded XRD patterns were subsequently analyzed using TOPAS 4.2 software and the International Centre for Diffraction Data (ICDD) Powder Diffraction Files (PDF2) database (2013). The lattice parameters were determined using TOPAS software and by performing full Rietveld refinement.

Third group of samples were used for XRD, light microscopy, electrical conductivity and hardness measurements. Samples were prepared by classic metallographic procedure without etching and sealed in the polymer. Microstructures of the samples were recorded on a light microscopy using (LOM) OLYMPUS GX41 inverted metallographic microscope. Electrical conductivity measurements were carried out using Foerster SIGMATEST 2.069 eddy instrument. Hardness of the samples was measured using Brinell hardness tester INNOVATEST, model NEXUS 3001 with indenter diameter of 1 mm and the pressing load 98,07 N.

3. Results and Discussion

For calculation of the phase equilibria in the ternary Ag-Bi-Ge system, thermodynamic data for binary sub-systems were used [18-20]. Thermodynamic parameters for the Ag-Ge system are from Wang et al. [18], for the Ag-Bi system from Zoro et al. [19] and for the Bi-Ge binary system from Chevalier [20]. Based on the results of our previous study and literature data, four different phases should appear in the ternary Ag-Bi-Ge system. One phase is liquid phase marked as a L phase, and in this phase all three elements Ag, Bi and Ge appear. Solid phases are (Ag), (Bi) and (Ge) solutions. In previous study it was determined that (Bi) and (Ge) solid solutions can dissolve neglected amount of other two elements while (Ag) solid solution can dissolve germanium (maximal ≈9 at. % at eutectic temperature) and bismuth (maximal ≈2.5 at. %). Crystallographic data about these solutions are summarized in Table 1.

(Ag) solid solution is stable from 0 to the 961.8 °C, and can dissolve maximal 9 at. % of germanium and 2.5 at. % of bismuth. This solid solution has a cubic crystal structure, with space group $Fm\overline{3}m$, and lattice parameters a=b=c=4.0861 Å. (Ge) solid solution is stable from 0 to the 938.2 °C. According to the literature, (Ge) solid solution does not dissolve silver or bismuth. (Ge) solid solution has cubic crystal structure with space group $Fd\overline{3}m$, and lattice parameters a=b=c=5.65675 Å. Third solid solution is (Bi), and this phase is stable from 0 to the 271.4 °C. It is rich with bismuth and according to the literature does not dissolve silver and germanium. (Bi) solid solution has rhombohedral crystal structure with space group $R\overline{3}m$, and lattice parameters a=b= 4.535 Å, and c= 11.814 Å.

Table 1. Crystallographic information of the solid phases of the Ag-Bi-Ge system [21-23].

Thermodynamic database name	Phase	Pearson symbol	Space group	Lattice parameters (Å)		Ref.
				a=b	*c*	
FCC_A1	(Ag)	c*F*4	$Fm\overline{3}m$	4.0861		[21]
DIAMOND_A4	(Ge)	c*F*8	$Fd\overline{3}m$	5.65675		[22]
RHOMBO_A7	(Bi)	h*R*2	$R\overline{3}m$	4.535±.002	11.814±.006	[23]

Table 2. EDS and XRD results of the ternary Ag-Bi-Ge samples annealed at 500 °C for four weeks.

N	Composition of samples x(at. %)	Determined phases		Compositions of phases x(at. %)			Lattice parameters l(10-10m)
		EDS	XRD	Ag	Bi	Ge	a=b=c
1	7.89 Ag	L		10.77±0.2	86.41±0.2	2.82±0.1	
	50.80 Bi	(Ge)	(Ge)	0.80±0.1	1.30±0.1	97.9±0.3	5.6532±0.0006
	41.31 Ge						
2	22.71 Ag	L		29.09±0.3	66.37±0.1	4.54±0.6	
	51.68 Bi	(Ge)	(Ge)	0.92±0.3	1.01±0.2	98.07±0.1	5.6538±0.0007
	25.61 Ge						
3	26.83 Ag	L		42.48±0.4	51.39±0.1	6.13±0.2	
	33.04 Bi	(Ge)	(Ge)	0.5±0.1	0.89±0.1	98.61±0.1	5.6552±0.0003
	40.13 Ge						
4	42.06 Ag	L		60.17±0.5	31.29±0.3	8.54±0.3	
	9.57 Bi	(Ge)	(Ge)	0.73±0.2	0.89±0.4	98.38±0.2	5.6549±0.0001
	48.37 Ge	(Ag)	(Ag)	91.67±0.3	1.73±0.5	6.6±0.1	4.1023±0.0005
5	59.97 Ag	L		62.85±0.3	28.85±0.4	8.3±0.1	
	19.97 Bi	(Ge)	(Ge)	0.98±0.5	1.13±0.5	97.89±0.2	5.6532±0.0004
	20.06 Ge	(Ag)	(Ag)	90.02±0.4	2.73±0.1	7.25±0.2	4.1029±0.0003
6	77.06 Ag	L		60.18±0.2	36.48±0.2	3.34±0.1	
	19.53 Bi	(Ag)	(Ag)	93.73±0.3	3.28±0.2	2.99±0.1	4.1019±0.0002

3.1. Isothermal section at 500 °C

Six ternary samples were annealed at 500 °C for four weeks and then analyzed by using SEM-EDS and XRD techniques. Experimental results are summarized in Table 2.

Within six investigated samples, three different phase regions were detected. Two of them are L+(Ge) and L+(Ag) two- phase regions and one is L+(Ge)+(Ag) three phase region. Samples 1, 2 and 3 belong to the same phase region L+(Ge). It is detected that liquid phase is rich with bismuth and silver, while phase (Ge) solid solution is rich with germanium. Samples 4 and 5 have same three phases in microstructure. Detected phases are L, solid solution (Ge) and solid solution (Ag). Two phases (L and solid solution (Ag)) are detected within the sample 6. It is noticeable that for the samples 1-6, content of the silver increases (sample 1, 7.89 at. % of the silver and sample 6, 77.06 at. % of the silver). Increase in silver content leads to the microstructural changes, so in microstructures of samples 1, 2 and 3 L and (Ge) solid solution are detected. In the sample 4, composition of silver is 42.06 at. %, and beside L and (Ge) phases, (Ag) solid solution is detected. This three phase region is detected in the sample 5, also. Sample 5 has 59.97 at. % of the silver. Content of silver in sample 6 is 77.06 at. % and in microstructure of sample 6, L and (Ag) solid solution phases are detected. In all samples L phase is stable while stability of (Ge) and (Ag) solid solutions changes depending on the composition of samples. So, in samples 1 to 5, (Ge) solid solution is stable and in sample 6 when composition of germanium inside sample is 3.41 at. % (Ge) solid solution is not stable. (Ag) solid solution is stable in the samples 4, 5 and 6. These samples are rich with silver.

Determined lattice parameters of the (Ag) and (Ge) solid solutions are compared with literature values [21,22]. Both solid solutions dissolve some amount of other two elements and determined lattice parameters are slightly changed for (Ag) to higher and for (Ge) to lower values, but difference is still too small in comparison to the literate values.

Four microstructures recorded by SEM are given in Figure 1.

Microstructures of samples 1 (Fig.1a)) and 3 (Fig. 1.b)) have same phases: L as a gray phase and (Ge) solid solution as a dark phase. Figure 1.c) presents micrograph of sample 5 with three visible phases: L as a light gray phase, solid solution (Ag) as a gray phase and (Ge) solid solution as a dark phase. Last presented micrograph is for sample 6, on which two phases are marked: L phase as a light gray phase and solid solution (Ag) as a gray phase.

Experimentally obtained results of EDS analysis summarized in Table 2 are compared with calculated isothermal section at 500 °C. Figure 2 shows comparison of EDS results and calculated isothermal section at 500 °C.

Calculated isothermal section at 500 °C has six different phase regions. Two are single phase regions (L and (Ag)), three are two-phase regions (L+(Ge), L+(Ag) and (Ge)+(Ag)), and one is three-phase region ((Ge)+(Ag)+L). Three of them are experimentally confirmed by analysis of the samples annealed at 500 °C. Two-phase region L+(Ge) has been experimentally confirmed within the samples 1, 2 and 3. In Figure 2, same color of symbol is used for marking EDS composition of sample and composition of detected phases in that sample.
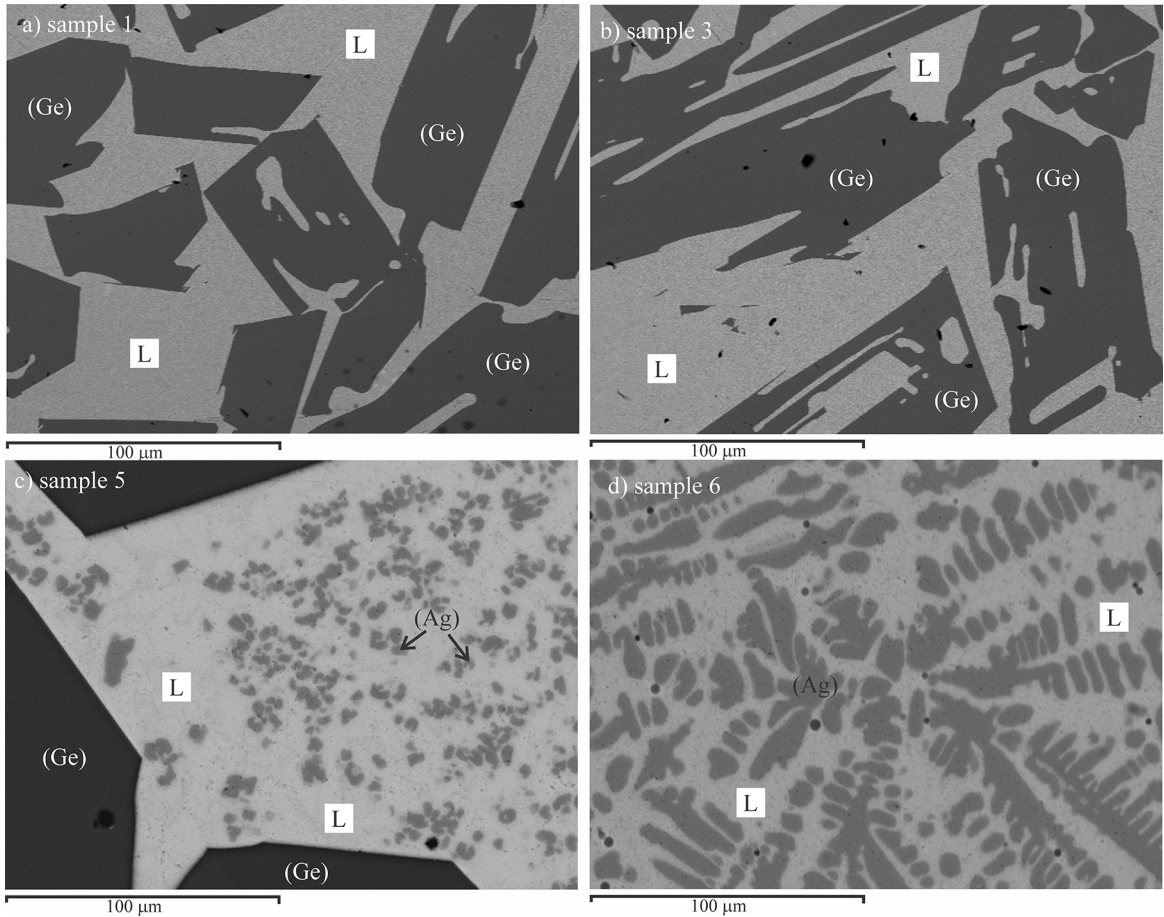
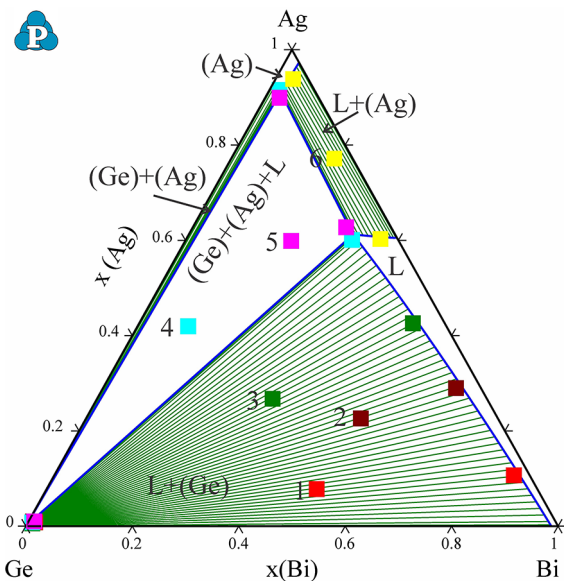**Figure 1.** SEM micrographs of a) sample 1, b) sample 3, c) sample 5 and d) sample 6.

Figure 2. Predicted isothermal section at 500 ºC compared with the experimental data.

By comparing EDS results of the phase compositions and calculated composition (calculated isothermal section) it is visible that calculated and experimental compositions of L and (Ge) phases in samples 1, 2 and 3 well reproduce each other. Three phase region (Ge)+(Ag)+L has been detected within the samples 4 and 5. By comparing EDS results with results of calculation it can be noticed that compositions of (Ge) solid solution agree well, compositions for L and (Ag) phase are slightly different but difference is very small, within 1 at. %. Sample 6 confirmed the existence of two-phase region L+(Ag) and composition of both experimentally detected phases are in good agreement with calculated results.

3.2. Isothermal section at 100 °C

Six ternary samples annealed at 100 °C are experimentally tested by using SEM-EDS and XRD methods. Obtained results of the tests are summarized in Table 3.

In all tested samples same three phases are detected. Tested samples are marked with numbers from 7 to 12, and composition of silver in samples increases from number 7 to 12.

Table 3. EDS and XRD results of the ternary Ag-Bi-Ga samples annealed at 100 ºC for six weeks.

N	Composition of samples x(at. %)	Determined phases		Compositions of phases x(at. %)			Lattice parameters 1(10^{-10}m)	
		EDS	XRD	Ag	Bi	Ge	a=b	c
7	62.03 Ag	(Ag)	(Ag)	98.05±0.3	0.75±0.4	1.2±0.2	4.0891±0.0003	
	22.81 Bi	(Bi)	(Bi)	0.05±0.2	98.92±0.1	1.03±0.5	4.5356±0.0002	11.8153±0.0002
	15.16 Ge	(Ge)	(Ge)	0.08±0.1	0.12±0.2	99.8±0.1	5.6563±0.0007	
8	55.23 Ag	(Ag)	(Ag)	98.03±0.1	1.02±0.2	0.95±0.2	4.0892±0.0006	
	18.65 Bi	(Bi)	(Bi)	0.80±0.1	98.71±0.1	0.49±0.2	4.5358±0.0005	11.8155±0.0007
	26.12 Ge	(Ge)	(Ge)	0.80±0.6	1.20±0.3	98.00±0.3	5.6543±0.0002	
9	32.80 Ag	(Ag)	(Ag)	98.32±0.2	0.87±0.4	0.81±0.1	4.0879±0.0008	
	18.62 Bi	(Bi)	(Bi)	0.31±0.2	99.07±0.5	0.62±0.5	4.5353±0.0003	11.8148±0.0005
	48.58 Ge	(Ge)	(Ge)	0.30±0.5	0.52±0.3	99.18±0.2	5.6559±0.0002	
10	32.18 Ag	(Ag)	(Ag)	98.25±0.4	1.08±0.3	0.67±0.3	4.0885±0.0005	
	34.60 Bi	(Bi)	(Bi)	0.51±0.4	99.03±0.2	0.46±0.5	4.5353±0.0001	11.8150±0.0008
	33.22 Ge	(Ge)	(Ge)	0.71±0.3	0.58±0.4	98.71±0.2	5.6551±0.0007	
11	9.33 Ag	(Ag)	(Ag)	98.72±0.2	0.18±0.2	1.1±0.1	4.0873±0.0005	
	32.22 Bi	(Bi)	(Bi)	0.51±0.1	98.31±0.2	1.18±0.2	4.5359±0.0002	11.8163±0.0002
	58.45 Ge	(Ge)	(Ge)	0.82±0.2	0.13±0.1	99.05±0.3	5.6556±0.0003	
12	7.28 Ag	(Ag)	(Ag)	98.31±0.1	0.92±0.2	0.77±0.5	4.0880±0.0001	
	65.86 Bi	(Bi)	(Bi)	0.81±0.3	98.52±0.2	0.67±0.2	4.5357±0.0004	11.8161±0.0001
	26.86 Ge	(Ge)	(Ge)	0.52±0.1	0.71±0.1	98.77±0.3	5.6552±0.0002	

Different compositions of the samples did not result in changes of detected phase constituents. Detected phases are (Ag), (Bi) and (Ge). Each phase is rich with one element and other two can be dissolved in small amounts of around 2 at. %. So detected solid solution (Ag) is rich with silver and amount of silver is in range from 98.03 at. % to the 98.72 at. % . Solid solution (Bi) is rich with bismuth and amount of bismuth is in range from 98.31 at. % to the 99.07 at. %. Third solid solution is (Ge), which is rich with germanium and its content ranges from 98.00 at. % to the 99.80 at. %.

XRD analysis also determined co-existence of three phases in the samples, same phases which were detected by EDS.

Lattice parameters of the detected solution phases are close to the literature values [21-23]. Composition of the samples and solid solutions did not influence significantly to the lattice parameters since in each sample same three phases are detected.

Figure 3 presents microstructures of samples 7 and 10.

On micrograph of the samples 7 and 10, three phases are visible (Ge) solid solution as a dark phase, (Ag) solid solution as a grey phase and (Bi) solid solution as a light grey phase.

Figure 4 presents calculated isothermal section at 100 °C compared with experimental EDS results given in Table 3.

As it is visible from Figure 4 calculated isothermal section at 100 ºC have just one three-phase region (Ge)+(Ag)+(Bi).
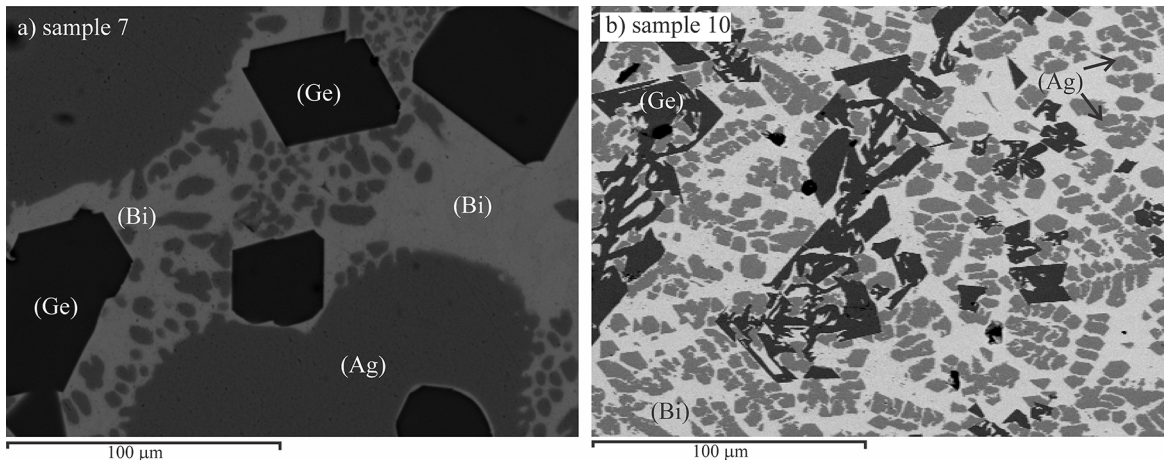
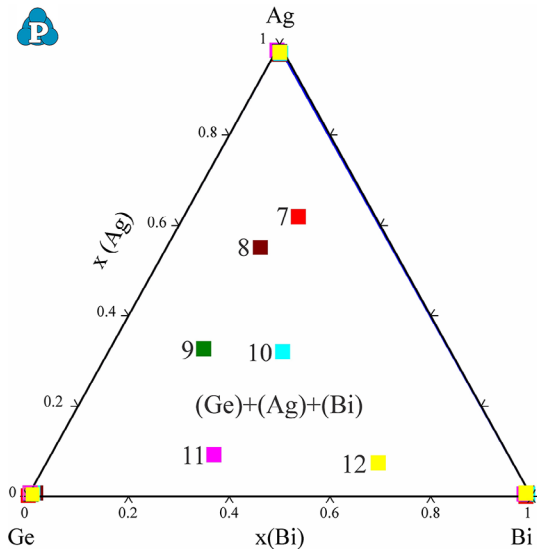**Figure 3.** SEM micrographs of a) sample 7 and b) sample 10.

Figure 4. Predicted isothermal section at 100 ºC compared with the experimental data.

3.3. Microstructural analysis

Twelve ternary samples are observed with light optical microscope. The compositions of ternary samples are positioned along three cross-sections Ag-BiGe, Bi-AgGe and Ge-AgBi. From every section four samples were prepared and marked with numbers from 13 to 24. First four samples are from Ag-BiGe section, samples 17-20 are from Bi-AgGe section and samples 21-24 are from Ge-AgBi section. Figure 5 presents calculated isothermal section at 25 ºC with marked composition of prepared samples.
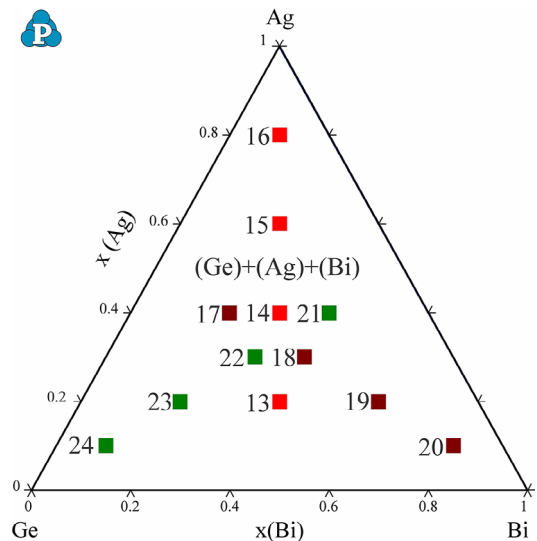

Figure 5. Predicted isothermal section at 25 ºC with marked compositions of tested alloys.

From isothermal section at 25 ºC only one three-phase region is visible. According to the calculation all investigated samples should have three phases (Ag), (Bi) and (Ge) in their microstructures. After observation of the samples in all 12 same three phases are visible. By using XRD method it is determined that three phases correspond to the (Ag), (Bi) and (Ge), same as calculated. Four microstructures of samples 15, 19, 21 and 24 are presented as an illustration in Figure 6.

In all given microstructures three phases can be noticed: solid solution (Ge) as a dark phase, solid solution (Ag) as a light phase and solid solution (Bi) as a grey phase.

3.4. Mechanical properties

By using Brinell hardness test, hardness values of twelve ternary alloys and three binary were determined. Hardness was measured at three different positions within the sample and summary of results is given in Table 4 together with literature values of hardness for pure elements [24].

Figure 7 presents a graphical presentation of the relationship between the Brinell hardness of the studied alloys from the three vertical sections and the alloy composition.

From Figure 7 and Table 4 it is noticeable that hardness of samples 13-23 is in the range from 40.23 (sample 17) to the 86.83 (sample 22) MN/m². Determined hardness for the sample 24 is 143.46 MN/m², which is significantly higher than others values. Such high hardness value can be connected with the very high content of germanium in this alloy (80 at.%).

By utilizing experimentally determined values of hardness given in Table 4 and software Desig Expert v.9.0.3.1 mathematical model of the dependence of the Brinell hardness on composition for the Ag-Bi-Ge alloys was developed.

None of Scheffe models (S-model) [25,26] did not satisfied Lack-of-fit tests. For calculations we used so-called Slack-Variable mixture models (SV-model) which are obtained by designating one mixture component as "Slack Variable". Reduced Quartic Slack Mixture model has been chosen. Mixture Component was Coding as L_Pseudo and Backward Elimination Regression with Alpha to Exit = 0.100 was used.

By recommendation of Cruz-Salgado [27] and Piepel et al. [28] for using SV-model , component C (Ge) is defined as the Slack variable. Analysis of variance confirms the adequacy of the Reduced Quartic Slack Mixture model (Table 5).

The F-value of the Model is 30.364 and it implies that the model is significant. In this case, all model terms are significant. R-squared and other statistics after the ANOVA have appropriate values which confirm the justification of the choice of the adopted mathematical model (Table 6). The "Lack of Fit F-value" of 1.72 implies the Lack of Fit is not significant relative to the pure error. There is a 13.46% chance that a "Lack of Fit F-value" this large could occur due to noise.
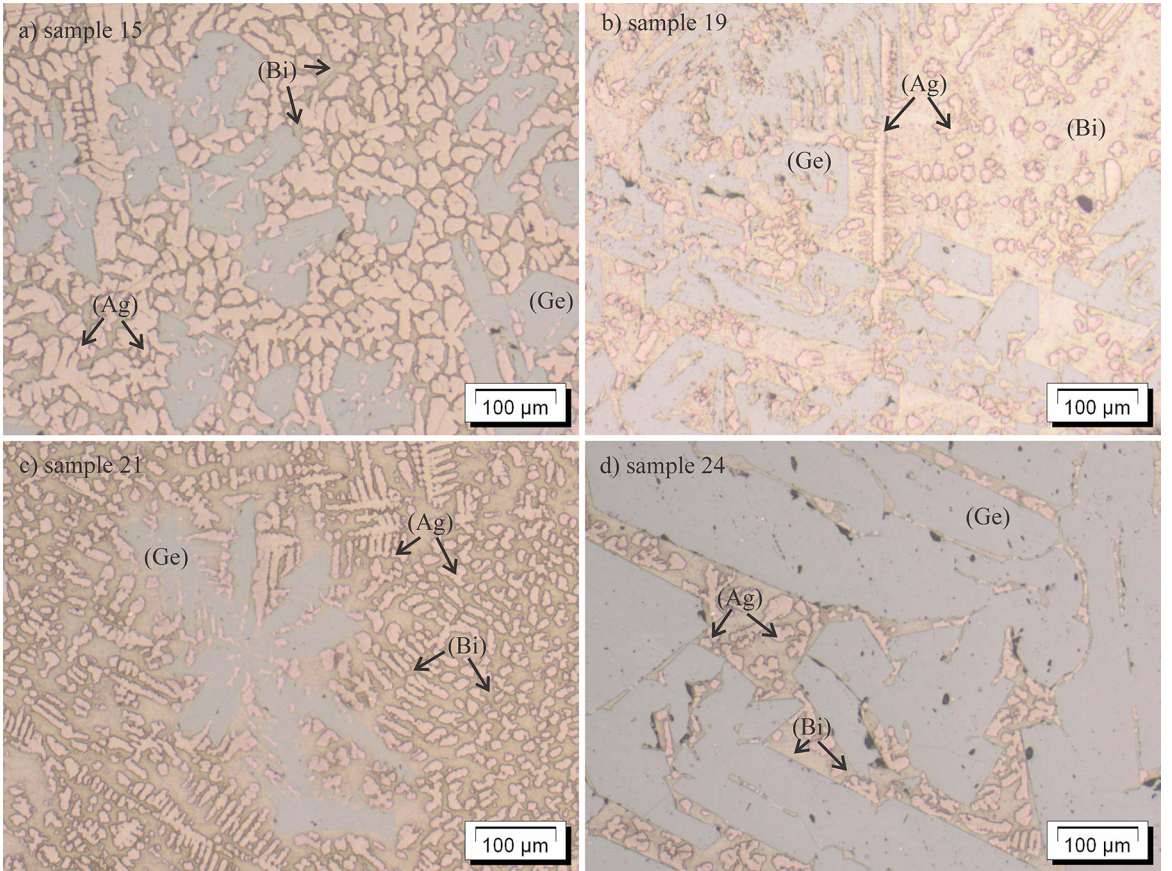
Figure 6. LOM micrographs of a) sample 15, b) sample 19, c) sample 21 and d) sample 24.

Table 4. Brinell hardness of ternary Ag-Bi-Ge alloys.

| N.	Mole fraction of components			Value (MN/m²)			Mean value (MN/m²)
	x(Ag)	x(Bi)	x(Ge)	1	2	3	
B1	0	0.5	0.5	117.4	124.2	122.6	121.4
13	0.2	0.4	0.4	56.2	59.0	86.8	67.3
14	0.4	0.3	0.3	61.0	103.1	67.4	77.16
15	0.6	0.2	0.2	66.6	52.2	72.4	63.73
16	0.8	0.1	0.1	113.5	62.8	61.0	79.1
	1	0	0		24.5		
B2	0.5	0	0.5	94	89.6	94.2	92.6
17	0.4	0.2	0.4	41.7	28.8	50.2	40.23
18	0.3	0.4	0.3	48.8	74.6	65.0	62.8
19	0.2	0.6	0.2	55.5	71.5	84.1	70.36
20	0.1	0.8	0.1	26.5	47.4	49.6	41.16
	0	1	0		94.2		
B3	0.5	0.5	0	60.6	63.4	64.1	62.7
21	0.4	0.4	0.2	38.4	59.6	32.1	43.36
22	0.3	0.3	0.4	66.2	78.3	116.0	86.83
23	0.2	0.2	0.6	83.2	71.5	104.7	86.46
24	0.1	0.1	0.8	98.8	184.4	146.9	143.46
	0	0	1				366.74
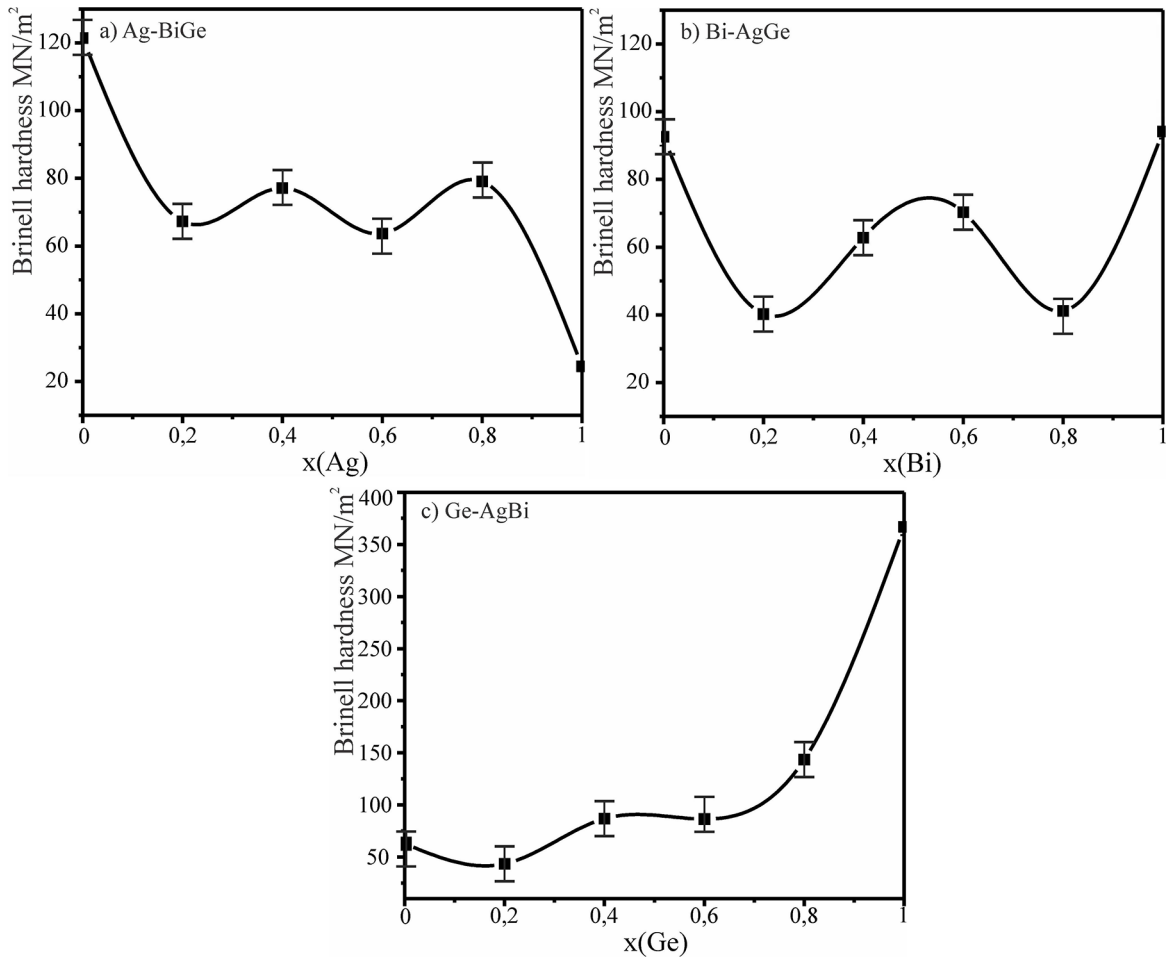
Figure 7. Mean value of Brinell hardness of the investigated Ag-Bi-Ge alloys with overall compositions along cross-sections: a) Ag-BiGe, b) Bi-AgGe, and c) Ge-AgBi.

Table 5. ANOVA for Reduced Quartic Slack Mixture model

Source	Sum of Squares	df	Mean Square	F Value	p-value Prob > F	
Model	114986.00	9	12776.22	30.364	< 0.0001	significant
A-Bi	22494.41	1	22494.41	53.460	< 0.0001	
B-Ag	52810.26	1	52810.26	125.509	< 0.0001	
AB	15837.80	1	15837.80	37.640	< 0.0001	
A^2	8148.49	1	8148.49	19.366	< 0.0001	
B^2	19216.99	1	19216.99	45.671	< 0.0001	
A^2B	4647.81	1	4647.81	11.046	0.0020	
A^3	4798.99	1	4798.99	11.405	0.0017	
A^3B	2521.65	1	2521.65	5.993	0.0191	
A^4	3672.15	1	3672.15	8.727	0.0054	
Residual	15989.22	38	420.77			
Lack of Fit	5026.74	8	628.34	1.720	0.1346	not significant
Pure Error	10962.49	30	365.42			
Cor Total	130975.22	47				

The "Pred R-Squared" of 0.8056 is in reasonable agreement with the "Adj R-Squared" of 0.8490 i.e. the difference is less than 0.2. "Adeq Precision" measures the signal to noise ratio. A ratio of 36.354 is greater than 4 and indicates an adequate signal.

Estimation of individual regression coefficients, Standard error and 95% confidence interval are shown in Table 7.

The final equation of the predictive model in terms of actual components is:

The diagnosis of the statistical properties of the assumed model found that the distribution of residuals are normal. After the applied Box-Cox procedure, the value of λ is 1.0, the optimum value of λ is 0.8 and the 95% confidence interval for λ (Low C.I.=0.39, High C.I.=1.13) contains the value 1.0, and it is not necessary to make correction of model. (Figure 8).

Iso-lines contour plot for Brinell hardness of alloys defined by equation 1 is shown in Fig. 9.

$$HB = 363.915813 - 2699.993x(Bi) - 746.89614x(Ag) + 4120.80065x(Ag) + 11154.0916x(Bi^2)$$
$$+ 406.523782x(Ag^2) - 14252.945x(Bi^2)x(Ag) - 18185.138x(Bi^3) + 15446.1015x(Bi^3)x(Ag) + 9460.0481x(Bi^4) \quad (1)$$

Table 6. R-squared and other statistics after the ANOVA

Std. Dev.	20.51	R-Squared	0.8779
Mean	81.28	Adj R-Squared	0.8490
C.V. %	25.24	Pred R-Squared	0.8056
PRESS	25460.59	Adeq Precision	36.3541

Table 7. Estimation of parameters for Reduced Quartic Slack Mixture model of Brinell hardness in ternary Ag-Bi-Ge system

| Component	Coefficient Estimate	df	Standard Error	95% CI Low	95% CI High
Intercept	363.92	1	18.53	326.41	401.42
A-Bi	-2699.99	1	369.27	-3447.55	-1952.44
B-Ag	-746.90	1	66.67	-881.86	-611.93
AB	4120.80	1	671.67	2761.08	5480.53
A^2	11154.09	1	2534.65	6022.97	16285.22
B^2	406.52	1	60.15	284.75	528.30
A^2B	-14252.95	1	4288.47	-22934.50	-5571.39
A^3	-18185.14	1	5384.73	-29085.94	-7284.33
A^3B	15446.10	1	6309.54	2673.10	28219.11
A^4	9460.05	1	3202.25	2977.44	15942.65
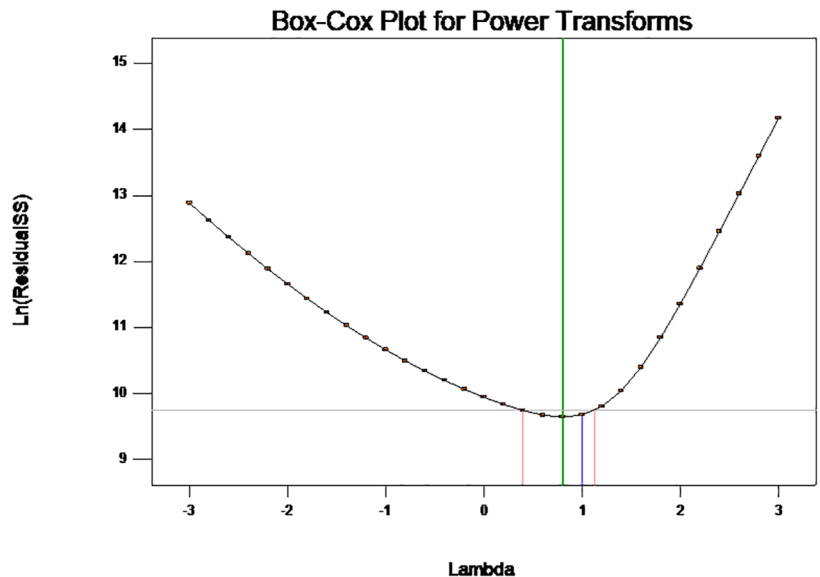
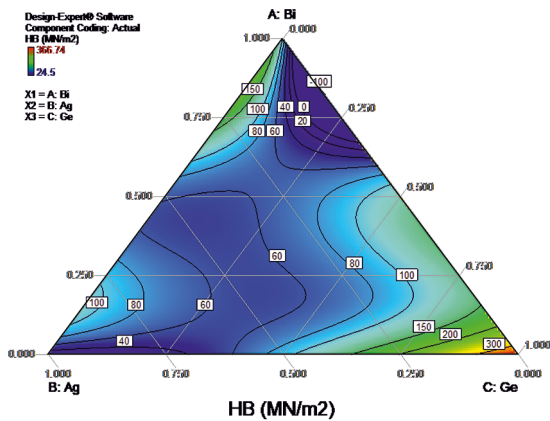**Figure 8.** The Box-Cox plot for power transformations

Figure 9. Calculated iso-lines of Brinell hardness in ternary Ag-Bi-Ge system with R^2 =0.8779.

To confirm whether the model can predict actual outcomes at the optimal settings Post Analysis was used. Additional four confirmation experiments with 3 runs are conducted at the optimal settings and obtained values of measured hardness by Brinell are given in Table 8. Also Confirmation Report are given in Table 9.

A two-sided interval bound with an alpha risk of α = 0.05 is specified. The mean responses from the confirmation experiments are compared with the prediction interval at the confirmation node. Since all averages of "n" observations from confirmation experiments are within the prediction interval (PI) of the confirmation node, so proposed model is confirmed (see the Confirmation Report - Table 9).

3.5. Electrical properties

Measurements of electrical conductivity were preformed on the same group of samples used for hardness determination. For all investigated samples electrical conductivity mesurements were repeated four times at different positions and obtained values for each measured point are given in Table 10. Beside measured values, Table 10 also includes calculated mean values and literature values of electrical conductivity for pure elements [29].

Figure 10 presents graphical presentation of results (mean value) given in Table 7 for a easier overview of the results.

Table 8. Brinell hardness of ternary Ag-Bi-Ge alloys for additional runs.

Mole fraction of components			Value (MN/m²)			Mean value (MN/m²)
x(Ag)	x(Bi)	x(Ge)	1	2	3	
0.333	0.333	0.333	54.1	73.6	63.5	63.73
0.6	0.2	0.2	54.6	70.9	65.1	63.53
0.2	0.6	0.2	62.2	60.4	78.5	67.03
0.2	0.2	0.6	98.7	74.4	82.3	85.13

Table 9. Confirmation report.

Point #	Predicted Mean	Predicted Median	Observed	Std Dev	n	SE pred	95% PI low	Data mena	95% PI high
1	63.405	63.405	-	20.5127	3	12.637	37.822	63.733	88.988
2	64.513	64.513	66.6	20.5127	3	14.228	35.710	63.533	93.316
3	59.862	59.862	55.5	20.5127	3	13.433	32.668	67.033	87.056
4	82.140	82.140	83.2	20.5127	3	14.228	53.337	85.133	110.943

Table 10. Electrical condyctivity of ternary Ag-Bi-Ge alloys.

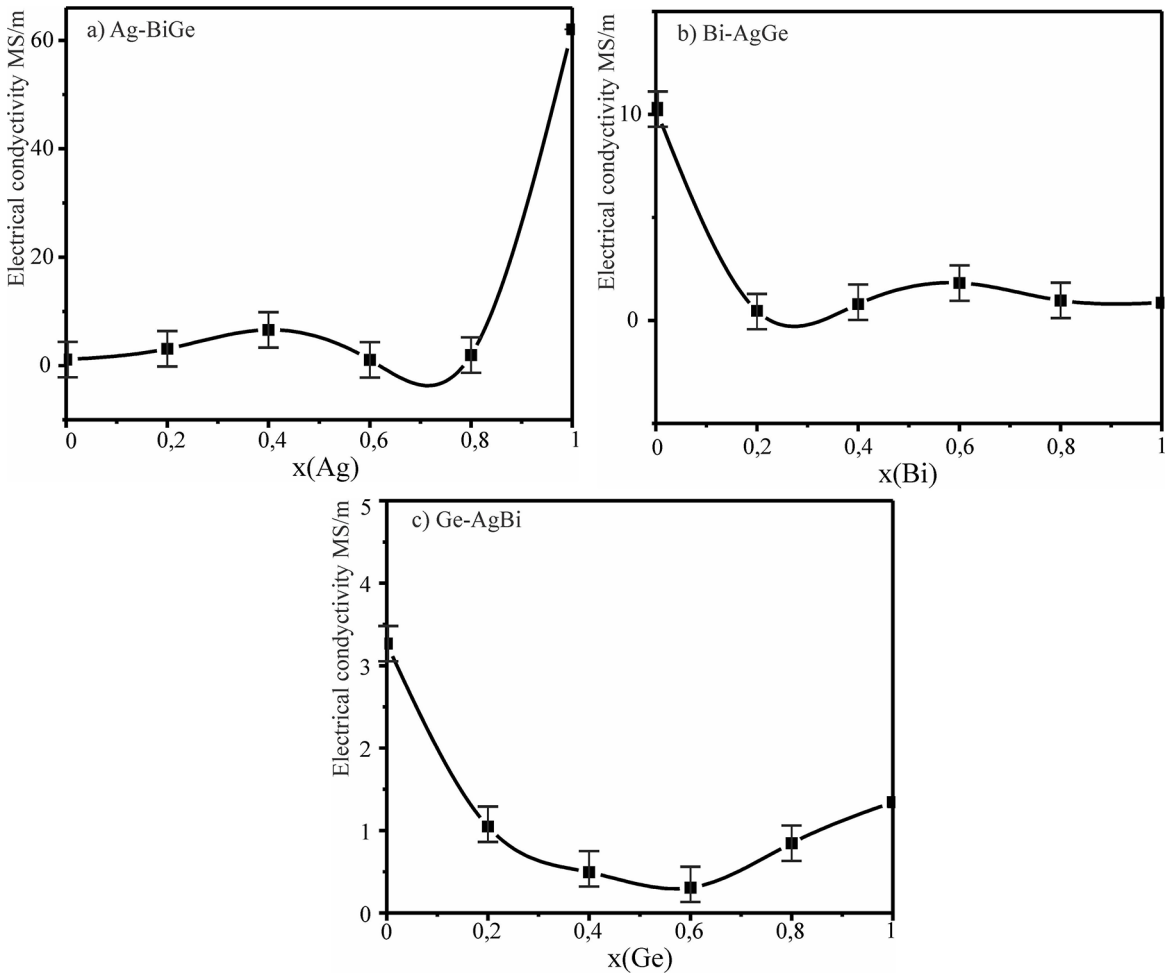| N	Mole fraction of components			Value (MS /m)				Mean value (MS/m)
	x(Ag)	x(Bi)	x(Ge)	1	2	3	4	
B1	0	0.5	0.5	1.24	1.012	1.12	1.355	1.124
13	0.2	0.4	0.4	0.3328	0.3057	0.3079	0.3051	0.3129
14	0.4	0.3	0.3	0.6459	0.6746	0.6472	0.6633	0.6578
15	0.6	0.2	0.2	1.013	1.136	1.064	1.144	1.089
16	0.8	0.1	0.1	1.908	1.951	1.984	1.899	1.936
	1	0	0		62			
B2	0.5	0	0.5	10.186	10.328	10.164	10.378	10.264
17	0.4	0.2	0.4	0.4676	0.4653	0.4802	0.4782	0.4728
18	0.3	0.4	0.3	0.8375	0.8358	0.83	0.6975	0.8002
19	0.2	0.6	0.2	1.842	1.8126	1.8288	1.8226	1.8265
20	0.1	0.8	0.1	0.9636	0.9689	0.9824	0.9795	0.9736
	0	1	0		0.867			
B3	0.5	0.5	0	3.314	3.244	3.268	3.242	3.267
21	0.4	0.4	0.2	1.055	1.041	1.052	1.047	1.049
22	0.3	0.3	0.4	0.4982	0.4835	0.4944	0.4978	0.4935
23	0.2	0.2	0.6	0.3059	0.3047	0.3056	0.3083	0.306
24	0.1	0.1	0.8	0.8639	0.869	0.8744	0.7807	0.847
	0	0	1					1.344

Figure 10. Electrical conductivity of the investigated Ag-Bi-Ge alloys with overall compositions along cross-sections: a) Ag-BiGe, b) Bi-AgGe, and c) Ge-AgBi.

Experimentally determined value of electrical conductivity in all ternary samples are close to each other, chemical composition does not contribute to change in electrical conductivity.

Based on experimental data given in Table 10, we tried to use same procedure as described for Brinell hardness to get mathematical model. None of Scheffe models (S-model) as well as Slack-Variable mixture models (SV-model) did not fill Lack-of-fit test and in this time it is not possible to obtain an adequate mathematical model. In future based on new experiments it will be possible to determine whether there is a dependence of the electrical conductivity on the fraction of the analyzed components.

4. Conclusions

The ternary Ag-Bi-Ge system has been experimentally investigated by using several experimental techniques. Two isothermal sections at 100 and 500 °C, were experimentally investigated by XRD and SEM-EDS techniques and thermodynamically extrapolated.

Experimental results were compared with calculated phase diagrams at 100 and 500 ºC and good agreement between data is reached. By EDS it is not detected ternary compound or large solubility of elements. Microstructural, hardness, electrical conductivity tests were performed on twelve ternary alloys and three binary alloys. On all twelve ternary alloys three phases in microstructures were detected, with XRD method it is confirmed that detected phases are (Ag), (Bi) and (Ge) solid solutions and by calculations of phase diagram at 25 °C it is confirmed that samples are from three-phase region (Ag)+(Bi)+(Ge). On same samples Brinell hardness and electrical conductivity were measured. Results of Brinell hardness and electrical conductivity were used for prediction of those properties along all composition of the ternary Ag-Bi-Ge system.

5. Acknowledgements

6. References

1. Chen YC, Rettner CT, Raoux S, Burr GW, Chen SH, Shelby RM, et al. Ultra-Thin Phase-Change Bridge Memory Device Using GeSb. In: Proceedings of the International Electron Devices Meeting; 2006 dec 1–13; San Francisco, CA. p. 777–780.

2. Raoux S, Wuttig M. *Phase Change Materials: Science and Applications*. New York: Springer-Verlag; 2009.

3. Raoux S, Ibm TJ. Phase Change Memory (PCM) materials and devices. In: Nishi Y, editor. *Advances in Nonvolatile Memory and Storage Technology*. Amsterdam: Woodhead Publishing; 2014. p. 161-199.

4. Siegrist T, Jost P, Volker H, Woda M, Merkelbach P, Schlockermann C, et al. Disorder-induced localization in crystalline phase-change materials. *Nature Materials*. 2011;10(3):202-208.

5. Kolobov AV, Tominaga J, Fons P. Phase-change memory materials. In: Kasap S, Capper P, editors. *Springer handbook of electronic and photonic materials*. Cham: Springer Handbooks; 2017. p. 1-11.

6. Yamada N, Ohno E, Akahira N, Nishiuchi K, Nagata K, Takao M. High speed overwritable phase change optical disk material. *Japanese Journal of Applied Physics*. 1987;26:61-66.

7. Ren G, Collins MN. Improved reliability and mechanical performance of Ag microalloyed Sn58Bi solder alloys. *Metals*. 2019;9(4):462-472.

8. Agrawal N, Sarkar M, Chawda M, Ganesan V. Carrier induced magnetism in dilute Fe doped $Ge1_{-x}Sb_x$ thin films. *Materials Chemistry and Physics*. 2013;143(1):330-335.

9. Kostov A, Zivkovic D, Zivkovic Z. Thermodynamic analysis of binary systems Ge–Ga and Ge–Sb. *Thermochimica Acta*. 1999;338(1-2):35-43.

10. Kalaba D, Sedmak A, Radakovic Z, Milos M. Thermomechanical modelling the resistance welding of PbSb alloy. *Thermal Science*. 2010;14(2):437-450.

11. Ren G, Wilding IJ, Collins MN. Alloying influences on low melt temperature SnZn and SnBi solder alloys for electronic interconnections. *Journal of Alloys and Compounds*. 2016;665:251-260.

12. Dalton E, Ren G, Punch J, Collins MN. Accelerated temperature cycling induced strain and failure behaviour for BGA assemblies of third generation high Ag content Pb-free solder alloys. *Materials and Design*. 2018;154(15):184-191.

13. Ren G, Collins MN. On the mechanism of Sn tunneling induced intermetallic formation between Sn-8Zn-3Bi solder alloys and Cu substrates. *Journal of Alloys and Compounds*. 2019;791:559-566.

14. Milisavljević D, Minić D, Premović M, Manasijević D, Balanović LJ. Experimental examination and thermodynamic description of the ternary Ag-Ge-Ga system. *Journal of Physics and Chemistry of Solids*. 2019;126:55-64.

15. Premović M, Manasijević D, Minić D, Živković D. Experimental investigation and thermodynamic prediction of the Ag–Ge–Sb phase diagram. *Journal of Alloys and Compounds*. 2014;610:161-168.

16. Premović M, Manasijević D, Minić D, **Živković** D. Study of electrical conductivity and hardness of ternary Ag-Ge-Sb system alloys and isothermal section calculation at 300 °C. *Kovové Materiály*. 2016;54(1):45-53.

17. Milisavljević D, Minić D, Premović M, Manasijević D, Ćosović V, Košanin N. Combined thermodynamic description and experimental investigation of the ternary Ag-Bi-Ge system. *International Journal of Thermophysics*. 2019;40:29.

18. Wang J, Liu YJ, Tang CY, Liu LB, Zhou HY, Jin ZP. Thermodynamic description of the Au–Ag–Ge ternary system. *Thermochimica Acta*. 2011;512(1-2):240-246.

19. Zoro E, Servant C, Legendre B. Thermodynamic assessment of the Ag–Au–Bi system. *Calphad*. 2007;31(1):89-94.

20. Chevalier PY. Thermodynamic evaluation of the Bi-Ge system. *Thermochimica Acta*. 1988;132:111-116.

21. Jette E, Foote F. Precision determination of lattice constants. *Journal of Chemical Physics*. 1935;3(10):605-615.

22. Cooper AS. Precise lattice constants of germanium, aluminum, gallium arsenide, uranium, sulphur, quartz and sapphire. *Acta Crystallographica*. 1962;15:578-582.

23. Cucka P, Barrett CS. The crystal structure of Bi and of solid solutions of Pb, Sn, Sb and Te in Bi. *Acta Crystallographica*. 1962;15:865-872.

24. Emsley J, *The Elements 3th edition*, Oxford University Press, Oxford UK; 1999. [access 2018 dec 25]. Available from: http://periodictable.com/Properties/A/BrinellHardness.al.html

25. Cornell JA. *Experiments* with *mixtures: designs, models, and the analysis of mixture* data. 3rd ed. New York: John Wiley & Sons; 2002.

26. Lazić ŽR. *Design of experiments in chemical engineering: practical guide*. Weiheim: Wiley-VCH Verlag; 2004.

27. Cruz-Salgado J. Selecting the slack variable in mixture experiment. *Ingeniería, Investigación y Tecnología*. 2015;16(4):613-623.

28. Greg FP, Dayton CH, Scott KC. *Slack-variable versus mixture modeling for mixture experiments: a definitive comparison*. 2018 Fall Technical Conference; 2018 oct 4; Richland, WA, USA: Pacific Northwest National Laboratory; 2018. p. 1-40.

29. Gray T. *Electrical conductivity of the elements*. Oxfordshire: Wolfram Research, Inc.; 1987. [access 2018 dec 25]. Available from: http://periodictable.com/Properties/A/ElectricalConductivity.an.html